

This is the accepted manuscript made available via CHORUS. The article has been published as:

α decay in intense laser fields: Calculations using realistic nuclear potentials

Jintao Qi, Tao Li, Ruihua Xu, Libin Fu, and Xu Wang

Phys. Rev. C **99**, 044610 — Published 22 April 2019

DOI: [10.1103/PhysRevC.99.044610](https://doi.org/10.1103/PhysRevC.99.044610)

Alpha decay in intense laser fields: Calculations using realistic nuclear potentials

Jintao Qi,¹ Tao Li,² Ruihua Xu,¹ Libin Fu,¹ and Xu Wang^{1,*}

¹*Graduate School, China Academy of Engineering Physics, Beijing 100193, China*

²*Beijing Computational Science Research Center, Beijing 100193, China*

We calculate the effect of intense laser fields on nuclear alpha decay processes, using realistic and quantitative nuclear potentials. We show that alpha decay rates can indeed be modified by strong laser fields to some finite extent. We also predict that alpha decays with lower decay energies are relatively easier to be modified than those with higher decay energies, due to longer tunneling paths for the laser field to act on. Furthermore, we predict that modifications to angle-resolved penetrability are easier to achieve than modifications to angle-integrated penetrability.

I. INTRODUCTION

The past few decades witness rapid advancements in intense laser technologies. The chirped pulse amplification technique [1] enables table-top Ti:sapphire lasers to have intensities exceeding one atomic unit (3.5×10^{16} W/cm²), opening the door to the rich area of strong-field atomic, molecular, and optical physics with novel nonperturbative phenomena such as multiphoton and above-threshold ionization [2, 3], high harmonic generation [4, 5], nonsequential double and multiple ionization [6, 7], attosecond physics [8–11], etc.

Even higher intensities can be achieved by larger laser systems of different kinds, for example, X-ray free electron lasers (XFELs) and the under-constructing extreme light infrastructure (ELI) of Europe. XFELs can be focused to reach peak intensities on the order of 10^{20} W/cm² [12]. ELI is designed to reach peak intensities above 10^{23} W/cm² [13, 14]. The laser electric field corresponding to such an intensity is comparable to the Coulomb field from the bare nucleus at a distance of order 10 fm. Direct influence on the nucleus may be possible from such an intense laser field. In fact, one of the major scientific goals of the ELI facility is to study laser-driven nuclear physics.

Direct light-nucleus interaction with much weaker light intensities has been realized using synchrotron radiations on the Mössbauer ⁵⁷Fe system. Using a grazing-incidence X-ray diffraction technique and a planar ⁵⁷Fe cavity, collective quantum optical effects have been demonstrated with photon energy 14.4 keV, such as single-photon superradiance [15], electromagnetically induced transparency [16], spontaneously generated coherence [17], Rabi oscillation [18], etc. On the other hand, the nuclei, as the media of X-ray pulse propagation, can be used to modify the properties of the X-ray pulse, such as the pulse shape [19] and the group velocity [20]. Theoretical proposals have also been made on single-photon entanglement [21], single-photon storage and phase modulation [22], nuclear battery using isometric transition [23–25], etc.

Non-resonant effects of intense laser fields on nuclear systems have also been reported in the literature. Among them possible influence of intense laser fields on nuclear alpha decay has received attention [26–29]. Widely accepted as a quantum tunneling process [30], alpha decay is expected to be modified in the presence of a strong laser field through modifying the potential barrier, on which quantum tunneling depends very sensitively. Indeed, existing works all predict such modifications.

To what degree an intense laser field, currently available or to be available in the forthcoming years, can influence alpha decay? This quantitative question, however, remains unanswered. Mişicu and Rizea numerically solve a time-dependent Schrödinger equation using a one-dimensional (1D) model nuclear potential [27, 28]. They focus on obtaining qualitative understandings instead of quantitative evaluations. Delion and Ghinescu [29] adopt a Kramers-Henneberger (KH) approximation [31, 32] to describe the laser-nucleus interaction. However, as will be explained in detail in the following section, the KH approximation is not valid to describe the laser-nucleus interaction. This explains why unreasonable predictions are made in Ref. [29] that the laser field greatly suppresses (by orders of magnitude) alpha decay along the polarization direction, where the laser electric field is the strongest, and greatly enhances (by orders of magnitude) alpha decay along the perpendicular direction, where no laser electric field is present.

The goal of the current article is to study the effect of intense laser fields on nuclear alpha decay quantitatively. To achieve this goal we need to start with a realistic and quantitative alpha-nucleus potential. In this work we use the potentials proposed by Igo [33], which have a simple analytical form and can be applied to a variety of nuclei. These potentials were obtained by fitting to alpha-nucleus scattering data. Our numerical results show that alpha decay can indeed be modified by strong external laser fields, to some small but finite extent. For example, with a laser intensity of 10^{24} W/cm², which is expected to be achievable in the forthcoming years with ELI, a modification of 0.1% to the alpha particle penetrability or the nuclear half life is predicted. Besides, the alpha decay is modified along the laser polarization direction, as would be expected reasonably. A somewhat surprising result is that alpha decays with lower decay energies are

*Electronic address: xwang@gscaep.ac.cn

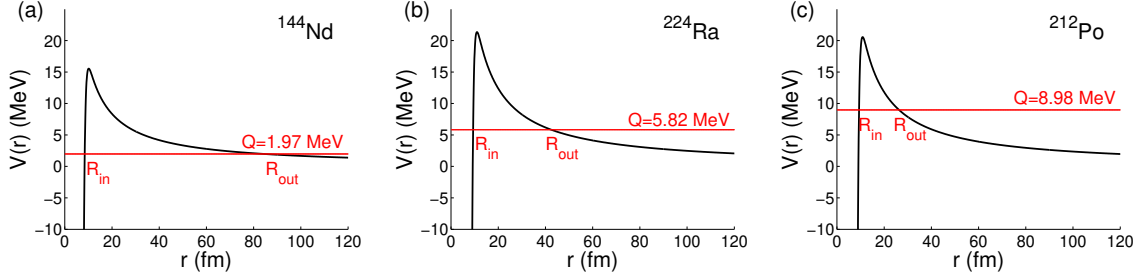


FIG. 1: Potentials between the alpha particle and the daughter nucleus, including the Igo alpha-nucleus potential and the Coulomb potential, for three nuclear elements (a) ^{144}Nd (b) ^{224}Ra and (c) ^{212}Po . The red horizontal line in each panel is the corresponding alpha decay energy Q , the intersections of which with the potential energy curve give the tunneling entrance point R_{in} and the tunneling exit point R_{out} .

relatively easier to be modified by external laser fields. This is due to longer tunneling paths under the potential barrier for the laser field to act on. We also explain that modifications to angle-resolved penetrability are easier to achieve than modifications to angle-integrated penetrability. The former modifications depend linearly on the laser electric field strength while the latter modifications depend quadratically on the laser electric field strength.

This article is organized as follows. In Section II we will introduce the methods that we use in our calculations. That includes the detailed form of the alpha-nucleus potentials, the form of the laser-nucleus interaction, and the method to calculate the alpha particle penetrability. Numerical results, analyses, and discussions are given in Section III. A conclusion is given in Section IV.

II. METHOD

A. The alpha-nucleus potential

The potential energy felt by the alpha particle from the residue (daughter) nucleus can be written as

$$V(r) = V_N(r) + V_C(r), \quad (1)$$

where r is the distance between the alpha particle and the daughter nucleus, $V_N(r)$ is a short-range nuclear potential and $V_C(r) = 2Z/r$ is the Coulomb repulsive potential. Z is the charge of the daughter nucleus.

Igo proposed a quantitative yet simple alpha-nucleus potential [33] by fitting to alpha-nucleus scattering data

$$V_N(r) = -1100 \exp \left\{ - \left[\frac{r - 1.17A^{1/3}}{0.574} \right] \right\} \text{ MeV}, \quad (2)$$

where r is in units of fm ($1 \text{ fm} = 10^{-15} \text{ m}$) and A is the mass number of the daughter nucleus. The potential is given in MeV.

Figure 1 shows the potential $V(r)$ for three representative alpha-decay elements, namely, ^{144}Nd , ^{224}Ra , and ^{212}Po . The decay energy Q for the three elements are

1.97, 5.82, and 8.98 MeV, respectively. Typical alpha-decay energies range within 1 MeV to 10 MeV, so the three elements chosen represent low-, medium-, and high-energy decays.

The decay energy Q is the sum of the kinetic energy of the alpha particle and the recoil energy of the daughter nucleus, and it can be obtained as

$$Q = \frac{A+4}{A} E_\alpha, \quad (3)$$

where E_α is the (detected) kinetic energy of the alpha particle, and A is the mass number of the daughter nucleus. Normally a very small electron-screening correction may be included due to energy loss of the alpha particle flying through the electron cloud of the atom. This small correction is not included in the current problem with the consideration that the electrons have been removed by the intense laser fields.

B. The laser-nucleus interaction

The interaction between the laser electric field and the nucleus is given in the length gauge as [27]

$$V_I(\vec{r}, t) = -Z_{eff} \vec{r} \cdot \vec{\epsilon}(t) = -Z_{eff} r \epsilon(t) \cos \theta, \quad (4)$$

where θ is the angle between \vec{r} and $\vec{\epsilon}(t)$, and $Z_{eff} = (2A - 4Z)/(A + 4)$ is an effective charge. This effective charge indicates the tendency of the laser electric field separating the alpha particle and the daughter nucleus. One sees that if $Z/A = 1/2$, then $Z_{eff} = 0$. That is, if the daughter nucleus has the same charge-to-mass ratio as the alpha particle, then the daughter nucleus and the alpha particle will move in concert in the laser field and the laser electric field does not have an effect of separating the two. For the three nuclear elements shown in Fig. 1, $Z_{eff} = 0.33$ for ^{144}Nd , 0.43 for ^{224}Ra , and 0.42 for ^{212}Po .

The neglect of the magnetic part of the laser field is justified by the fact that the alpha particle moves much slower than the speed of light. Assuming a kinetic energy of 10 MeV, one gets an alpha particle speed of 2.2×10^7

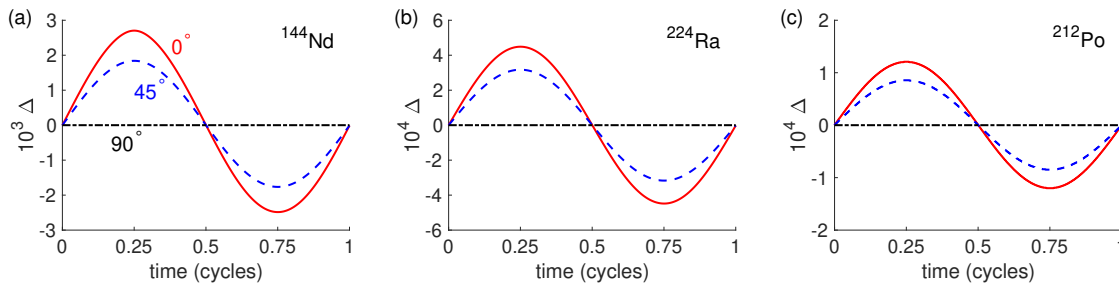


FIG. 2: Time-dependent modifications to the alpha particle penetrability, seen from three spatial angles, namely, $\theta = 0^\circ$ (red solid), 45° (blue dashed), and 90° (black dash dotted). The same three nuclear elements are used as in Fig. 1. The peak intensity used is 10^{24} W/cm² for all the three elements.

m/s, about 7% the speed of light. Therefore the effect of the magnetic field on the alpha particle is expected to be much smaller than that of the electric field.

C. The quasistatic approximation

The size of a typical nucleus is on the order of 1 fm. From a classical picture, the alpha particle oscillates back and forth within the nucleus. The frequency of this oscillation can be estimated to be $\sim 2 \times 10^7 \text{ m} \cdot \text{s}^{-1} / 2 \text{ fm} = 10^{22}$ Hz. Each time the alpha particle hits the potential wall, it has a small chance (which is called the penetrability) of tunneling out. If it does, we may estimate how much time the alpha particle needs to tunnel through the potential barrier. Referring Fig. 1, the length of the potential barrier for the alpha particle to tunnel through is on the order of 10 fm. So the alpha particle needs about 10^{-21} s to travel through the potential barrier. This time is much smaller than an optical cycle of strong lasers. For the 800 nm near-infrared laser of ELI, one optical cycle is 2.6×10^{-15} s. For 10 keV X-ray lasers, one optical cycle is 4×10^{-19} s. Therefore during the time that the alpha particle penetrates through the potential barrier, the change of the laser field is negligible and the laser field can be viewed as static. This is the quasistatic approximation. In strong-field atomic physics, such approximation is routinely used describing tunneling ionization of atoms [34–37].

It is obvious that the Kramers-Henneberger approximation [31, 32] is not valid here. The KH approximation says that when the laser frequency is much higher than the particle oscillating frequency, the particle responds dominantly to the cycle-averaged laser field value (like our eyes' response to light). This high-frequency condition of validity for the KH approximation is well known in the literature [38, 39]. Applying the KH approximation to the laser-assisted alpha decay process has led to unreasonable predictions by Delion and Ghinescu [29], as mentioned previously in the Introduction.

D. The penetrability of the alpha particle

Based on the quasistatic approximation, the penetrability of the alpha particle through the potential barrier can be calculated using the Wentzel-Kramers-Brillouin (WKB) method as

$$P(\theta, t) = \exp \left(-\frac{2}{\hbar} \int_{R_{in}}^{R_{out}} \sqrt{2\mu[V(r) - Q + V_I(r, \theta, t)]} dr \right), \quad (5)$$

where $V(r)$ and $V_I(r, \theta, t)$ are given in Eqs. (1) and (4), respectively. The laser polarization is assumed to be along the z axis and θ denotes the direction of alpha emission, with respect to the +z axis. Understanding from the classical picture, the alpha particle oscillates back and forth inside the nucleus, and every time it hits the potential wall, it has a probability of $P(\theta, t)$ to tunnel out.

In this article we mainly look into the relative change of the penetrability induced by the laser field. The relative change of the penetrability is defined as

$$\Delta = \frac{P(\varepsilon) - P(\varepsilon = 0)}{P(\varepsilon = 0)}, \quad (6)$$

where ε is the laser field strength. Δ is also understood as a function of the emission angle θ and time t .

III. RESULTS AND DISCUSSIONS

A. Laser-induced modifications to the penetrability

First we show that the penetrability of the alpha particle can indeed be modified by strong external laser fields. Figure 2 shows time-dependent modifications to the penetrability seen from three spatial angles with respect to the +z direction, namely, $\theta = 0^\circ$ (red solid curves), $\theta = 45^\circ$ (blue dashed curves), and $\theta = 90^\circ$ (black dash-dotted curves). The same three nuclear elements are used as in Fig. 1. The modifications are strongest along $\theta = 0^\circ$, i.e., when the alpha emission direction is parallel to the laser polarization direction. No modifications

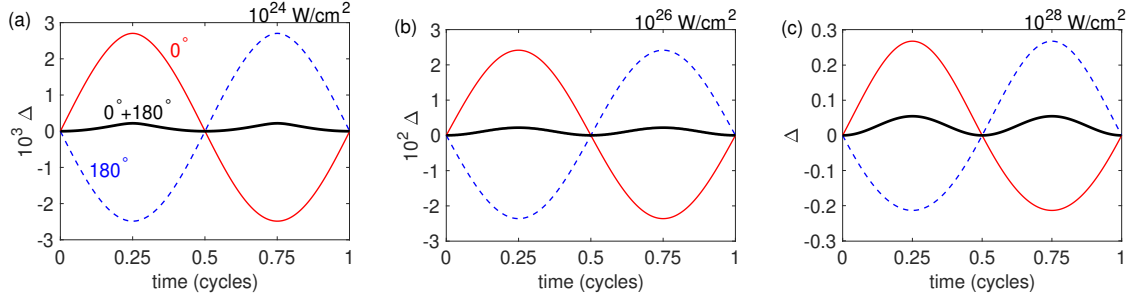


FIG. 3: Relative changes of the penetrability P seen from $\theta = 0^\circ$ and from $\theta = 180^\circ$, for three different laser intensities, namely, 10^{24} W/cm 2 (a), 10^{26} W/cm 2 (b), and 10^{28} W/cm 2 (c). The nuclear element used here is ^{144}Nd . Positive-negative asymmetry between 0° and 180° can be more clearly seen from the sum of the two, as shown by the thick black curve in each panel.

are seen along $\theta = 90^\circ$, when the emission direction is perpendicular to the laser polarization direction.

A peak intensity of 10^{24} W/cm 2 is used for all the three nuclear elements. This intensity is expected to be achieved by ELI in the forthcoming years. One sees that modifications to the alpha penetrability are on the order of 0.1% for ^{144}Nd and of 0.01% for ^{224}Ra or ^{212}Po . The same amount of modifications are made to the nuclear half lives.

It may seem unexpected at first that ^{144}Nd , with a lower decay energy than ^{224}Ra and ^{212}Po , is relatively easier to be modified by external laser fields. This is a consequence of the tunneling mechanism. ^{144}Nd has a longer tunneling path for the laser field to act on, as shown in Fig. 1, and the potential from the laser electric field is proportional to this path length.

B. Laser potential as a perturbation to the alpha-nucleus potential

Compared to the potential energy between the alpha particle and the daughter nucleus, the laser potential has much smaller magnitudes, even with an intensity of 10^{24} W/cm 2 . We can gain insights into the laser-modification process by treating the laser potential as a perturbation to the alpha-nucleus potential.

Let us start from the penetrability exponential given in Eq. (5) and write it in the following form

$$P(\theta, t) = \exp \left\{ -\frac{2\sqrt{2}\mu}{\hbar} \int_{R_{in}}^{R_{out}} \sqrt{V_0 + V_I} dr \right\} \quad (7)$$

$$= \exp \left\{ -\frac{2\sqrt{2}\mu}{\hbar} \int_{R_{in}}^{R_{out}} \sqrt{V_0} \sqrt{1 + \frac{V_I}{V_0}} dr \right\} \quad (8)$$

where for convenience $V_0(r) \equiv V(r) - Q$. By assuming

$|V_I| \ll |V_0|$, we have the following Taylor expansion

$$P(\theta, t) = \exp \left\{ -\frac{2\sqrt{2}\mu}{\hbar} \int_{R_{in}}^{R_{out}} \sqrt{V_0} \right. \\ \left. \times \left(1 + \frac{V_I}{2V_0} - \frac{V_I^2}{8V_0^2} + \dots \right) dr \right\} \quad (9)$$

$$\approx \exp \left(\gamma^{(0)} + \gamma^{(1)} + \gamma^{(2)} \right) \quad (10)$$

$$= \exp \left(\gamma^{(0)} \right) \exp \left(\gamma^{(1)} + \gamma^{(2)} \right) \quad (11)$$

$$\approx P(\varepsilon = 0, \theta, t) \left(1 + \gamma^{(1)} + \gamma^{(2)} \right) \quad (12)$$

where $\gamma^{(0)}$, $\gamma^{(1)}$, and $\gamma^{(2)}$ are defined as

$$\gamma^{(0)} = -\frac{2\sqrt{2}\mu}{\hbar} \int_{R_{in}}^{R_{out}} \sqrt{V_0(r)} dr \quad (13)$$

$$\gamma^{(1)} = \varepsilon(t) \frac{\sqrt{2}\mu Z_{eff} \cos \theta}{\hbar} \int_{R_{in}}^{R_{out}} \frac{r dr}{\sqrt{V_0(r)}} \quad (14)$$

$$\gamma^{(2)} = \varepsilon^2(t) \frac{\sqrt{2}\mu Z_{eff}^2 \cos^2 \theta}{4\hbar} \int_{R_{in}}^{R_{out}} \frac{r^2 dr}{V_0^{3/2}(r)} \quad (15)$$

Note that $\gamma^{(0)}$ is independent of the laser electric field, $\gamma^{(1)}$ is proportional to $\varepsilon(t)$, and $\gamma^{(2)}$ is proportional to $\varepsilon^2(t)$.

C. 0° versus 180°

When there is no laser field, alpha emission to the direction $\theta = 0^\circ$ is the same as that to $\theta = 180^\circ$. When the laser electric field is on and pointing to 0° , the penetrability to the same direction increases, but at the same time the penetrability to the opposite direction (180°) decreases.

For intensities with which $\gamma^{(2)}$ is negligible, the response of the penetrability to the laser electric field is linear. This means that the amount that P increases along 0° is equal to the amount that P decreases along 180° . The same argument can be made to other emission directions as well. Then there will be no net gain in

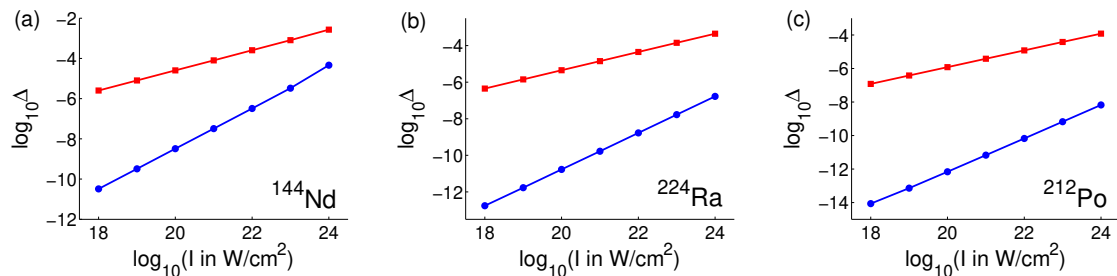


FIG. 4: Angle-resolved (red squares) and angle-integrated (blue circles) modifications to the alpha decay penetrability, as a function of laser intensity. Both Δ and the intensity I are plotted in the logarithmic scale, with which both curves are linear. The red (square) curves have slope 0.5, due to a linear dependency on the laser field strength. The blue (circle) curves have slope 1.0, due to a quadratic dependency on the laser field strength.

the total alpha decay rate integrating over all emission directions. Only for higher intensities with which $\gamma^{(2)}$ is not negligible, does the total alpha decay rate increase. This can be seen from Eq. (15) that $\gamma^{(2)}$ is always positive so both 0° and 180° contribute positively to the decay rate. Therefore modifying the angle-integrated total decay rate requires much higher laser intensities than modifying the angle-resolved decay rates. The former is a second-order process in laser field strength, whereas the latter is a first-order process in laser field strength.

Figure 3 shows the comparison between the modification to the alpha decay rate seen from 0° and from 180° , for three different intensities, namely, 10^{24} W/cm², 10^{26} W/cm², and 10^{28} W/cm². The nuclear element used is ^{144}Nd . One can see that for the lower two intensities, 0° and 180° look quite symmetric from naked eyes, although small asymmetries do exist, as can be seen from the sum of the two angles (the thick black curve in each panel). For the relatively high intensity shown in panel (c), obvious positive-negative asymmetry can be seen, due to appreciable $\gamma^{(2)}$ values with this intensity.

D. Angle-resolved versus angle-integrated modifications

Figure 4 shows the angle-resolved (red squares) and angle-integrated modifications (blue circles) to the alpha decay penetrability. The relative modification Δ and the laser intensity I are plotted in the logarithmic scale, therefore both curves are linear. The slope of the red curves is 0.5, due to a linear dependency on the laser electric field, while the slope of the blue curves is 1.0, due to a quadratic dependency on the laser electric field. Similar linear dependencies have also been predicted in Ref. [26] with 1D nuclear models and various nuclear species.

As analyzed in the previous subsection, for the intensities used in the current article, as well as laser intensities available in the near future, the response of the alpha decay to the external laser field is dominantly linear. Observing from a particular spatial angle, the modification

to the alpha penetrability depends (almost) linearly on the laser field strength. The linear response cancels if the angle-integrated modifications are considered, leaving the quadratic response dominating.

E. Possible experimental tests

In this subsection we propose an experimental scheme to test the predicted modifications to the alpha-decay penetrability by intense laser fields.

We propose to use elliptically polarized laser fields to observe the laser-induced modifications. Elliptical polarization (EP) is able to “throw” alpha particles emitted at different times to different spatial angles, rendering the modifications free from time averaging. For if alpha particles emitted at two times arrive at the same position of the detector, and the increase to the alpha-decay penetrability at one time balances the decrease at the other time, then the time-integrated signal at the detector will not discriminate modifications of individual times. This is what would happen using linearly polarized laser fields. The problem can be cured using EP. This property of EP has been exploited in strong-field atomic physics to extract ionization information that is otherwise hidden with linear polarization [40–43].

An elliptically polarized laser field is illustrated in Fig. 5 (a). The x-y plane is the polarization plane with the x direction the major direction, and the ellipticity value is 0.5. The electric field $E(t)$ rotates along the polarization ellipse. The effect of the elliptically polarized laser field on the alpha-emission process is twofold. First, the laser field adds an additional velocity (basically the vector potential) to the alpha particle, and the value of the additional velocity is determined by the time of emission. An example is illustrated in Fig. 5 (b). Without the laser field, the alpha particle has equal probabilities emitting to all directions with the same velocity, forming a circle on the asymptotic velocity distribution. With the laser field, the circular velocity distribution will be shifted by an amount determined by the time of emission. Second, the laser field modifies the probability emitting to differ-

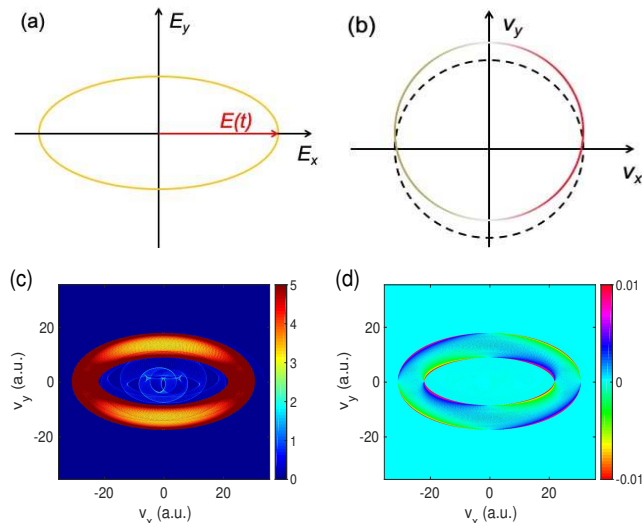


FIG. 5: (a) An elliptically polarized laser field. The field $E(t)$ rotates along the polarization ellipse. (b) Asymptotic velocity distribution of the emitted alpha particle without (dashed circle) and with (solid grey circle) the laser field. With the laser field, the position of the circle will be shifted and the distribution over the circle will no longer be uniform. (c) Simulated alpha particle velocity distribution using a trapezoidal laser pulse. The velocities are in atomic units and the color scale is in arbitrary units. (d) Difference in the velocity distribution if there were no modifications to the penetrability. The color-scale units are the same as in (c).

ent directions. The probability of emission to the right can be different from that to the left, for example, as illustrated in Fig. 5 (b).

The above argument on a single time step applies to all time steps during the laser pulse. Different time steps lead to different velocity shifts and penetrability modifications. Integrating over a laser pulse (assuming an intensity of 10^{24} W/cm² and a 100-cycle, or 267 fs, trapezoidal pulse with a 2-cycle linear ramping on and a 2-cycle linear ramping off), the asymptotic velocity distribution is simulated as in Fig. 5 (c). If there were no modifications to the alpha-decay penetrability, this velocity distribution would be slightly different, and the difference is shown in Fig. 5 (d). This difference, compared to the raw data, is roughly two orders of magnitude smaller in absolute values. The advantage of using EP can be seen: increase and decrease in the penetrabilities appear in different parts of the velocity distribution without overlapping. If a pattern similar to Fig. 5 (d) could

be identified by comparing an experimental distribution and a theoretical one assuming no modification to the penetrability, then the theory of the current article could be verified.

IV. CONCLUSION

We report in this article a combined theoretical and numerical study on the possible influences of strong laser fields on the nuclear alpha decay process. We use realistic and quantitative alpha-nucleus potentials and aim at obtaining quantitative evaluations of the laser influences.

We first show that the alpha penetrability (or equivalently the nuclear half life) can indeed be modified by strong laser fields to some small but finite extent, with laser intensities expected to be achievable in the forthcoming years especially with the under-constructing ELI facility. We also predict that alpha decays with lower decay energies are easier to be modified than those with higher decay energies, due to longer tunneling paths for the laser electric field to act on. This is a somewhat counterintuitive result.

We point out that compared to the alpha-nucleus potential, the additional laser potential is weak, even with the highest laser intensities achievable in the near future. The response of alpha decay to the laser field is shown to be restricted to the lowest two orders (linear and quadratic). Angle-resolved alpha penetrability is shown to be a first-order process, depending linearly on the laser field strength. Whereas angle-integrated alpha penetrability is shown to be a second-order process, depending quadratically on the laser field strength, or linearly on the laser field intensity. Future experiments investigating laser-modified alpha decay processes should start with angle-resolved observables. An experimental scheme based on elliptically polarized laser fields is proposed.

Acknowledgement

We acknowledge funding support from China Science Challenge Project No. TZ2018005, China NSF No. 11774323 and No.11725417, National Key R&D Program No. 2017YFA0403200, and NSAF No. U1730449.

References

-
- [1] D. Strickland and G. Mourou, *Opt. Commun.* **56**, 219 (1985).
 - [2] P. Agostini, F. Fabre, G. Mainfray, G. Petite, and N. Rahman, *Phys. Rev. Lett.* **42**, 1127 (1979).
 - [3] G. G. Paulus, W. Nicklich, H. Xu, P. Lambropoulos, and H. Walther, *Phys. Rev. Lett.* **72**, 2851 (1994).
 - [4] A. McPherson, G. Gibson, H. Jara, U. Johann, T. S. Luk, I. A. McIntyre, K. Boyer, and C. K. Rhodes, *JOSA B* **4**, 595 (1987).
 - [5] M. Ferray, A. L'Huillier, X. F. Li, L. A. Lompre, G. Main-

- fray, and C. Manus, J. Phys. B **21**, L31 (1988).
- [6] B. Walker, B. Sheehy, L. F. DiMauro, P. Agostini, K. J. Schafer, and K. C. Kulander, Phys. Rev. Lett. **73**, 1227 (1994).
 - [7] S. Palaniyappan, A. DiChiara, E. Chowdhury, A. Falkowski, G. Ongadi, E. L. Huskins, and B. C. Walker, Phys. Rev. Lett. **94**, 243003 (2005).
 - [8] F. Krausz and M. Ivanov, Rev. Mod. Phys. **81**, 163 (2009).
 - [9] K. Zhao, Q. Zhang, M. Chini, Y. Wu, X. Wang, and Z. Chang, Opt. Lett. **37**, 3891 (2012).
 - [10] J. Li, *et al.*, Nat. Commun. **8**, 186 (2017).
 - [11] T. Gaumnitz, A. Jain, Y. Pertot, M. Huppert, I. Jordan, F. Ardana-Lamas, and H. Jakob Wörner, Opt. Express **25**, 27506 (2017).
 - [12] P. H. Bucksbaum and N. Berrah, Physics Today **68**, 7, 26 (2015).
 - [13] D. Ursescu, O. Tesileanu, D. Balabanski, G. Cata-Danil, C. Ivan, I. Ursu, S. Gales, N. V. Zamfir, Proc. SPIE **8780**, 87801H-1 (2013).
 - [14] C.A. Ur et al., Nucl. Instr. Meth. B **355**, 198 (2015).
 - [15] R. Röhlsberger, K. Schlage, B. Sahoo, S. Couet, and R. Ruffer, Science **328**, 1248 (2010).
 - [16] R. Röhlsberger, H. Wille, K. Schlage, and B. Sahoo, Nature **482**, 199 (2012).
 - [17] K. P. Heeg, et al., Phys. Rev. Lett. **111**, 073601 (2013).
 - [18] J. Haber, X. Kong, C. Strohm, S. Willing, J. Gollwitzer, L. Bocklage, R. Ruffer, A. Pálffy, and R. Röhlsberger, Nat. Photonics **11**, 720 (2017).
 - [19] F. Vagizov, V. Antonov, Y. V. Radeonychev, R. N. Shakhmuratov, and O. Kocharovskaya, Nature **508**, 80 (2014).
 - [20] K. P. Heeg, et al., Phys. Rev. Lett. **114**, 203601 (2015).
 - [21] A. Pálffy, C. H. Keitel, and J. Evers, Phys. Rev. Lett. **103**, 017401 (2009).
 - [22] W.-T. Liao, A. Pálffy, and C. H. Keitel, Phys. Rev. Lett. **109**, 197403 (2012).
 - [23] W.-T. Liao, A. Pálffy, and C. H. Keitel, Phys. Lett. B **705**, 134 (2011).
 - [24] W.-T. Liao, S. Das, C. H. Keitel, and A. Pálffy, Phys. Rev. Lett. **109**, 262502 (2012).
 - [25] W.-T. Liao, A. Pálffy, and C. H. Keitel, Phys. Rev. C **87**, 054609 (2013).
 - [26] H. M. Castañeda Cortés, C. Müller, C. H. Keitel, and A. Pálffy, Phys. Lett. B **723**, 401 (2013).
 - [27] Ș. Mișicu and M. Rizea, J. Phys. G **40**, 095101 (2013).
 - [28] Ș. Mișicu and M. Rizea, Open Phys. **14**, 81 (2016).
 - [29] D. S. Delion and S. A. Ghinescu, Phys. Rev. Lett. **119**, 202501 (2017).
 - [30] G. Gamow, Z. Physik **51**, 204 (1928).
 - [31] H. A. Kramers, *Collective Scientific Papers* (North-Holland, Amsterdam, 1956), p.262.
 - [32] W. C. Henneberger, Phys. Rev. Lett. **21**, 838 (1968).
 - [33] G. Igo, Phys. Rev. Lett. **1**, 72 (1958).
 - [34] M.V. Ammosov, N. B. Delone, and V. P. Krainov, Sov. Phys. JETP **64**, 1191 (1986).
 - [35] T. Brabec, M. Y. Ivanov, and P. B. Corkum, Phys. Rev. A **54**, R2551 (1996).
 - [36] J. Chen, J. Liu, L. B. Fu, and W. M. Zheng, Phys. Rev. A **63**, 011404 (2000).
 - [37] G. L. Yudin and M. Y. Ivanov, Phys. Rev. A **63**, 033404 (2001).
 - [38] M. Gavrila and J. Z. Kaminski, Phys. Rev. Lett. **52**, 613 (1984).
 - [39] M. Pont and M. Gavrila, Phys. Rev. Lett. **65**, 2362 (1990).
 - [40] P. Eckle, A. N. Pfeiffer, C. Cirelli, A. Staudte, R. Dörner, H. G. Muller, M. Büttiker, and U. Keller, Science **322**, 1525 (2008).
 - [41] X. Wang and J. H. Eberly, Phys. Rev. Lett. **103**, 103007 (2009).
 - [42] X. Wang and J. H. Eberly, Phys. Rev. Lett. **105**, 083001 (2010).
 - [43] X. Wang, J. Tian, and J. H. Eberly, Phys. Rev. Lett. **110**, 073001 (2013).